SEVENTH EUROPEAN ROTORCRAFT AND POWERED LIFT AIRCRAFT FORUM

Paper No. 68

CFC DRIVE SHAFT AND GFC COUPLING FOR THE TAIL ROTOR OF THE BO 105

C.M. Herkert
D. Braun
K. Pfeifer

Messerschmitt-Bölkow-Blohm GmbH
Munich, Germany

September 8 - 11, 1981

Garmisch-Partenkirchen
Federal Republic of Germany

Deutsche Gesellschaft für Luft- und Raumfahrt e.V.

Goethestr.10, D-5000 Köln, F.R.G.

CFC DRIVE SHAFT AND GFC COUPLING FOR THE TAIL ROTOR OF THE BO 105

C.M. Herkert
D. Braun
K. Pfeifer

Messerschmitt-Bölkow-Blohm GmbH
Munich, Germany

Abstract

A fibre composite drive shaft and coupling for the BO 105 tail rotor are currently under development at MBB. The work described is sponsored by the Ministery of Defense of the F.R.G. The metal drive shafts and couplings for both drive system sections - long and short drive system section for the tail rotor - are intended to be improved regarding mass and cost aspects. These were the reasons why composites have been taken into account as a good solution for reducing manufacturing costs, number of single parts and life cycle costs.

This paper concentrates on requirements for design, analytical evaluation and testing, manufacturing and economical aspects of the fibre composite solution for this drive shaft system. Different design concepts are presented. Manufacturing technologies and tool design are discussed before the analytical evaluation is given and compared with static test results. Dynamic test results on both, short and long drive shafts are shown and discussed in terms of comparable flight hours. Finally a mass comparison between metal and composite solution is followed by the discussion of cost effectiveness and economical aspects. The paper closes with the presentation of the next programme steps.

1. Introduction

The existing production tail rotor drive system is composed of three shafts (Figure 1): short drive shaft attached to the main gearbox, short drive shaft attached to the tail rotor and long drive shaft as connection between these two short shafts. This long drive shaft is supported by four bearings on the tail boom of the helicopter. Each connection point of either long or short metal shaft is formed by a metal coupling. Flanges of couplings and shafts are of titanium alloy. They are bolted to a number of metal lamella which form the coupling. In the same way, the flange is attached to the metal tube (Figure 2).

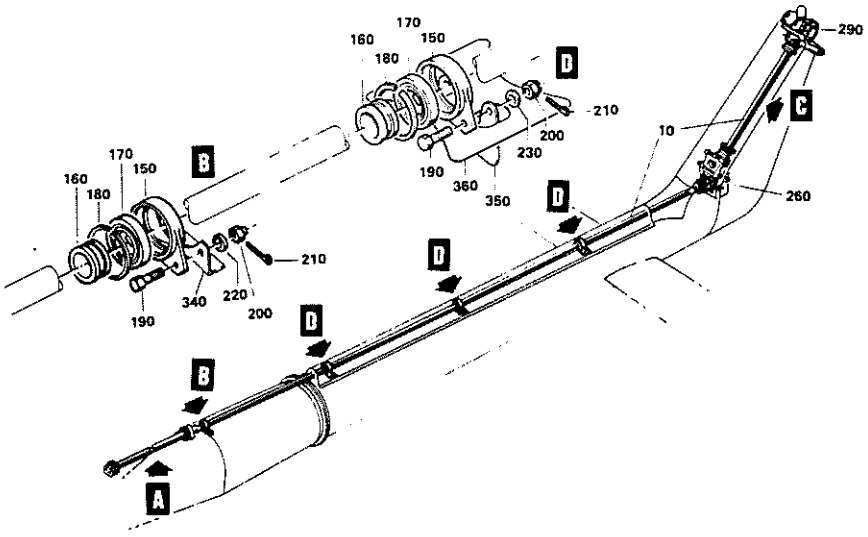

Figure 1 Complete drive shaft system BO 105

At the beginning of the work, main emphasis was placed upon the reduction of the number of bearings for the long drive shaft. This led to a carbon fibre composite (CFC) shaft containing high tensile fibres. The outer diameter of this shaft was determined to approximately 50 mm with a necessary wall thickness of 2.5 mm. The aim of the whole programme is to test the selected composite solution over a certain period during flight. Therefore, one was forced to go back to the parts geometry of the existing BO 105. Thus one had to take the four bearings for the long drive shaft and the outer diameter of the tube of 32 mm. This led to a CFC solution with high modulus fibres TORAY M40-3000x40A incorporated in epoxy resin and to a wall thickness of 5 mm. The metal flanges of the shaft and the metal couplings are replaced by GFC parts.

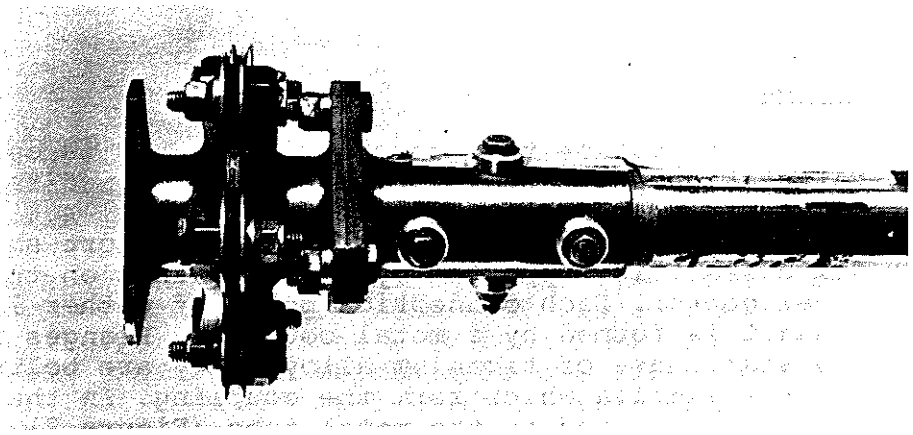

Figure 2 Metal version of drive shaft end

2. Requirements

The requirements can be devided in three areas:

- -general
- - shaft
- - coupling and flanges

2.1 General aspects

The designed composite version has to match all the interface points of the metal version. Furthermore, it has to be avoided vibration coupling with other systems. In addition to this mechanical and geometrical aspects, environmental aspects e.g. corrosion resistance and resistance against oil and grease according to MIL-L-23699 (0-156) and MIL-G-81322 (G-395) must be regarded for all materials used. The system should be usable in a temperature range of $-57°C \leq T \leq +80°C$ and should have no necessity for maintenance before the inspection at 1200 flight hours. Furthermore, it should have a growth capacity for increasing engine power starting with 103 kW at 2460 rev/min. These technical requirements are enlarged by economical ones which ask for remarkable reduction in mass, manufacturing costs, and number of parts.

2.2 Drive shaft

In order to avoid vibration coupling with adjacent components the drive shafts must show:

- -first natural frequency in torsion of about 4.3 Hz
- -first natural frequency in bending of about 64.1 Hz
- -outer diamter 32 mm due to the interface to the bearings
- -capability of carrying shear loads (from each bearing) in the range of 1000 N

Besides all this, the strength requirements in the interface areas to flanges and bearings have to be met.

2.3 Coupling and flange

The coupling must be capable to allow an axial displacement of $\pm$ 1.3 mm, an axial deflection of at least 1° and withstand a maximum torsional moment of 390 Nm. In comparison to the metal coupling, the stiffness values of the composite coupling should be increased for torsional loading and decreased for bending, tension and compression loading.

Composite flanges should act as connection members between drive shafts and couplings and drive shafts and metal flanges of the gearboxes.

3. Predesign and different concepts

For the total system two ways in design were followed. The first way was to try to minimize the number of bearings for the long drive shaft by varying the outer diameter of the shaft. This led to a construction with three bearings instead of four of the production version and an outer diamter of the CFC tube of 50 mm instead of 32 mm. Because of the fixation to the tail-boom of the BO 105 for later flight tests this work was only finished in software inclusive analytical evaluation. Some results are shown in Figure 3.

3.1 Drive shaft and flange connection

The design work of the drive shaft mainly consisted of selecting the best fibre type or fibre combination. This selection was done in a close interaction with the analytival evaluation described in chapter 4. The tube of the drive shaft is composed of fibres embedded in an epoxy matrix and forming unidirectional chords for the required bending stiffness. These chords are incorporated in a $\pm 45°$ filament wound tube which gives the necessary torsional stiffness to the part. Depending on the outer diameter of the tube and the chosen fibre type, different mechanical behaviour could be observed. The wall thickness varied from 4 to 6 mm. Figure 3 shows the essential values for different combinations. In order to be able to compare these with the metal versions the values of the latter are given at the top of the table.At the bottom of the table one can see that by increasing the diameter to 50 mm the use of high strength fibres is acceptable.

The next point that had to be focussed was the connection of flange and tube. Seven different concepts were looked at.

	Value / Material		Density [g/cm³]	Younge' Modulus [N/mm²]	Shear Modulus [N/mm²]	Mass [kg]	ult. bending Strength [N/mm²]	ult. torsional Strength [N/mm²]	ultimate deflection [mm]
O.D. 32mm	Metal	SANDVIK S R 10	7.8	200000	84000	5.8	950		»50
	Composite 50 vol-% fibers	Toray M40-3000x40A CY209/HT972	1.49	61600	35600	2.7	387	417	106.1
		UCC Thornel 75S CY209/HT972	1.51	86400	51000	2.5	187	218	36.6
		Toray T300-3000x40A CY209/HT972	1.47	42000	22600				
		Toray M40-3000x40A Kevlar 49-III CY209/HT972	1.47	61500	32600				
O.D. 50mm		Toray T300-3000x40A CY209/HT972	1.47	42000	22600	2.2	521	494	

Figure 3 Comparison of mechanical behaviour of different composite solutions versus metal solution

The range reached from single lapped outer conical bonding over octagonal conical bonding to normal bolting. Figure 4 shows some of the regarded connection possibilities. These can be devided

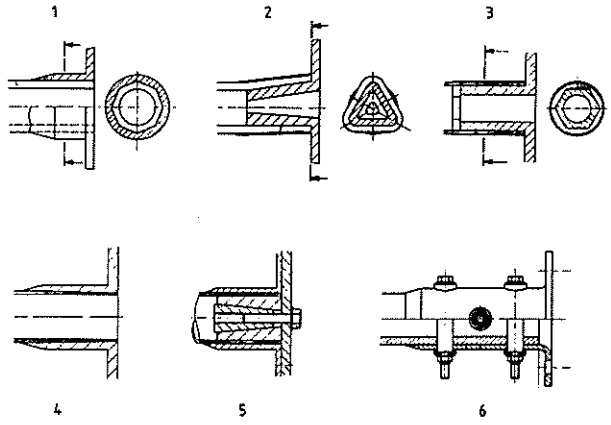

Figure 4 Connection possibilities of tube and flange

in disconnectable and permanent ones. For the long drive shaft at least one side must be disconnectable because of the necessity of bearing replacement whereas the short shafts can contain permanent conncections of flanges and shaft at both ends.

3.2 Coupling

Due to the requirement of large coupling deflections glass fibre fabric composite with a plain weave was selected as coupling material. Different concepts of the couplings concentrated on the geometrical design and on possibilities of integrating the connecting flanges into the coupling. The offered solutions reach from a filament wound coupling element with integrated flanges (6) over two-part prepreg moulded couplings with integrated flanges (1) to a single disc coupling (5). All these variations are shown in Figure 5.

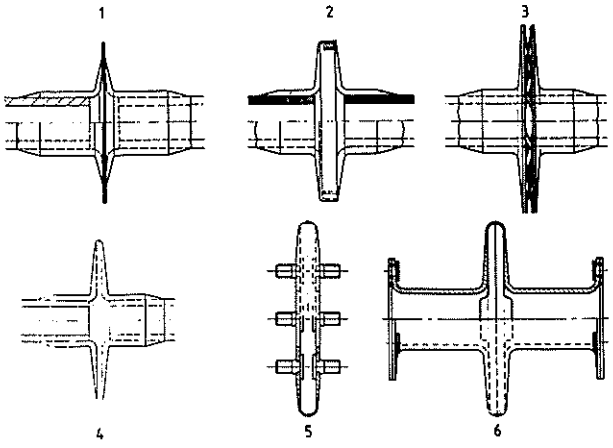

Figure 5
Coupling variations in GFC

The detailed design and the manufacturing of the selected concepts is discussed in chapter 6 and 7. The connection of the coupling flange to the tube is alternatively solved by a fail safe bonding (conical octagonal shape) or by bearing strength in the composite by bolts.

4. Analytical evaluation

4.1 Drive shaft and complete system

Dynamic characteristics

An essential criterion for the layout of the helicopter tail rotor drive shaft is the determination of the critical rotational speeds. In order to be sure that no dangerous operating conditions may occur it has to be guaranteed that the critical bending speeds, as well as the critical torsional speeds of the driving system, lie within sufficient distances below or above the operating speed (sub-critical and over-critical operation respectively) and do not coinicide with integral multiples thereof.

The theoretical evaluation of the critical speeds for different concepts of CFC tail rotor drive shafts is done by use of suitable idealized equivalent dynamical systems.

Neglecting mass and inertia of shafts, couplings and gear wheels, the critical torsional speed is computed by use of the system shown in Figure 6. The rotating energy of the tail rotor is relatively small compared to that of the main rotor. Therefore, the tail rotor driving system can be regarded with sufficient accuracy as an isolated torsional system which is clamped at the main gearbox output.

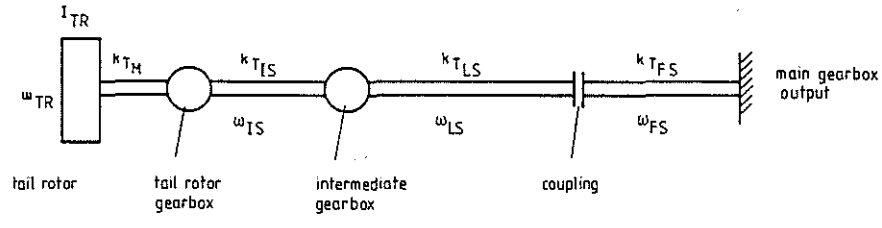

Figure 6 Equivalent dynamical system for the calculation of the critical torsional speed of the long tail rotor drive shaft

The mechanical model for the calculation of the critical bending speeds of the long tail rotor shaft is shown in Figure 7. The shaft is idealized by a beam with uniformly distributed

mass. The bearings on the tail boom are simulated by adequate local springs and point masses. The flexible shaft couplings are substituted by corresponding torsional springs.

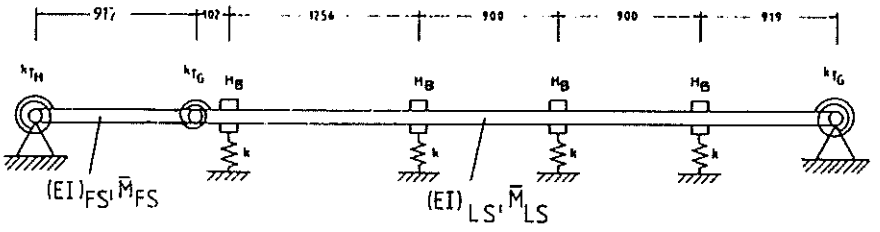

Figure 7 Equivalent dynamical system for the calculation of the critical bending speeds of the tail rotor drive shaft

The results for the critical torsional speeds and for the critical bending speeds (1st and 2nd mode) of several composite tail rotor drive shafts are summarized in Figure 8. For compa-

material	weight/length kg/m	torsional stiffness Nm^2	bending stiffness Nm^2	critical torsional speed referred to the operating speed	critical bending speed referred to the operating speed	
					1. mode	2. mode
Toray HM(M40A)/PRD	0.624	2610	2460	0.110	1.7	2.15
Toray HT (T300)	0.624	1810	1680	0.095	1.5	2.1
Toray HM (M40A)	0.630	2850	2460	0.113	1.7	2.15
Thornel 75 S	0.640	4080	3450	0.130	1.9	2.3
SANDVIK 5 R 10	1.480	3375	4390	0.116	1.6	2.1

Figure 8 Critical torsional and bending speeds for several tail rotor drive shafts

rison, the values for the conventional stainless steel production version of the B0 105 helicopter are given. In addition, the bending mode shapes for the selected TORAY HM drive shaft and for the stainless steel drive shaft are shown in Figure 9 and Figure 10.

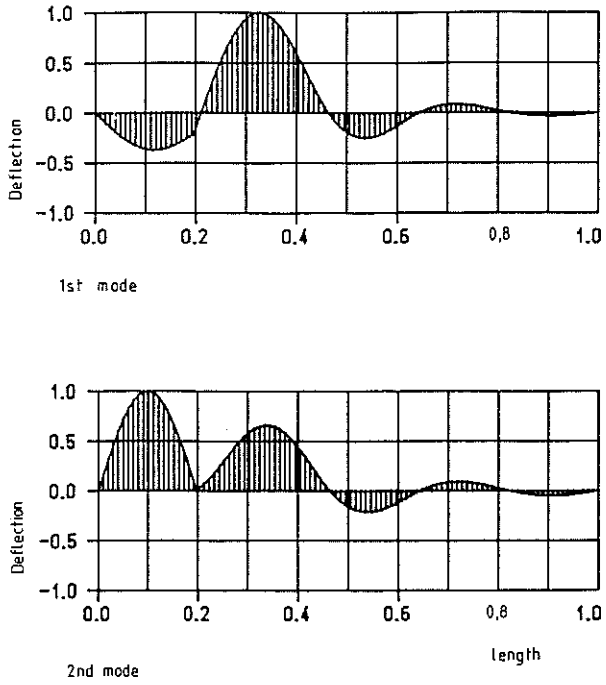

Figure 9 Bending mode shapes for the CFC prototype tail rotor drive shaft (TORAY HM)

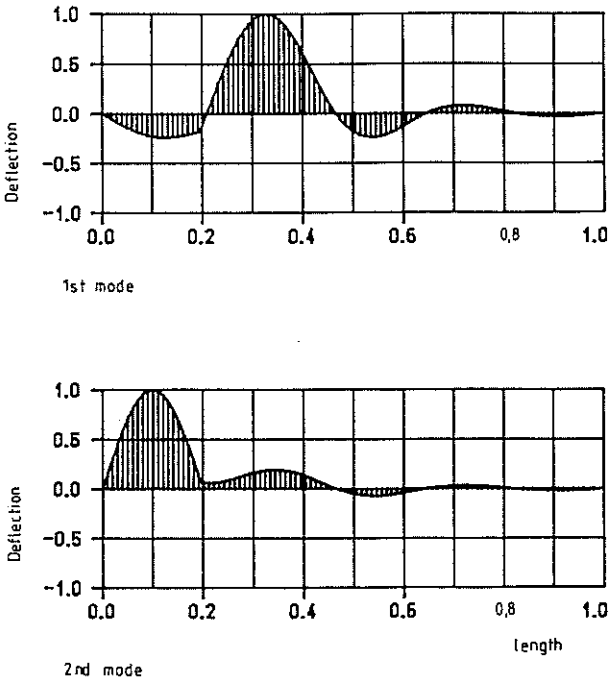

Figure 10 Bending mode shapes for the production tail rotor drive shaft (stainless steel)

Stiffness and stress analysis

The laminate layup in Figure 11 was used for the calculation with different kinds of fibres which rendered the selection of the most profitable fibre type.

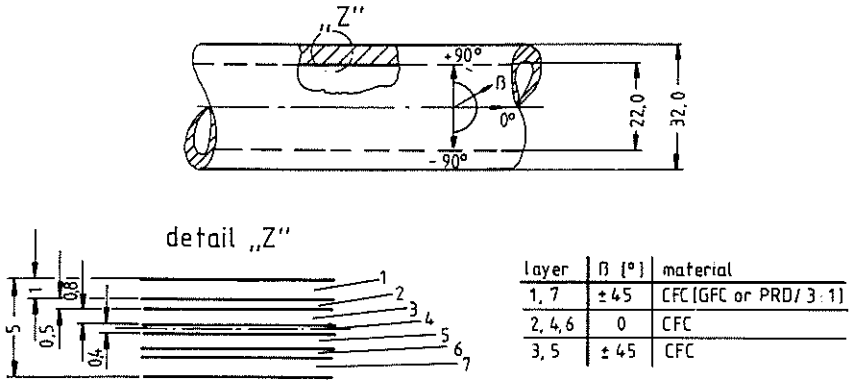

layer	ß [°]	material
1, 7	±45	CFC (GFC or PRD/ 3 : 1)
2, 4, 6	0	CFC
3, 5	±45	CFC

Figure 11 Geometry and laminate layup of the drive shaft

The unidirectional fibres carry the bending moments and the longitudinal loads whereas the ±45° glass fibre plies carry the torsional moments and the shear loads. Figure 12 shows the results of the calculation.

Material of the drive shaft	specific density of the laminate ϱ [g/cm³]	Young's modulus 10^3 [N/mm²]	shear modulus 10^3 [N/mm²]	bending stiffness [Nm²]	torsional spring stiffness GI/l [Nm/rad]	equivalent spring stiffness D_{eq} [Nm/rad]	bending eigenfrequency f_B [Hz] 1st harm.	2nd harm.	torsional eigenfrequency f_T [Hz]
E-Glas	1,85	1,88	0,86	752	179	202	37,5	62,2	2,3
PRD 49 III	1,33	2,67	1,36	1068	276	299	51,8	83,8	2,8
Grafit HT	1,50	4,38	2,43	1751	493	490	61,7	86,2	3,6
Grafit HM	1,58	5,65	3,19	2259	647	608	69,4	87,7	4,1
Toray HT (T300)	1,47	4,20	2,26	1679	459	462	61,1	86,1	3,5
Toray HM (M40A)	1,49	6,16	3,56	2463	723	661	70,4	87,8	4,2
Thornel 75 S	1,51	8,64	5,10	3454	1035	854	80,0	93,4	4,8
hybrid composites									
Grafit HT/E-Glas	1,54	4,39	2,22	1755	450	454	61,1	86,1	3,5
Grafit HM/E-Glas	1,60	5,64	2,88	2255	585	562	68,5	87,5	3,9
Toray HT (T300)/E-Glas	1,51	4,16	2,08	1671	422	431	60,3	85,9	3,4
Toray HM (M40A)/E-Glas	1,53	6,16	3,19	2463	647	608	69,9	87,7	4,1
Thornel 75 S/E-Glas	1,55	8,63	5,10	3450	917	854	80,0	92,6	4,6
Grafit HT/PRD	1,48	4,38	2,29	1751	465	467	62,1	86,3	3,6
Grafit HM/PRD	1,55	5,62	2,94	2247	597	571	69,5	87,8	3,9
Toray HT (T300)/PRD	1,45	4,17	2,15	1667	436	443	61,2	86,1	3,5
Toray HM (M40A)/PRD	1,47	6,15	3,26	2459	662	618	70,8	88,0	4,1
Thornel 75 S/PRD	1,49	8,61	4,59	3442	932	795	80,1	93,7	4,6

Figure 12 Summary of the calculated results: eigenfrequency of bending and torsion versus type of fibre material

By knowing the stiffnesses and the loads, the resulting strains can be computed.

Torsional angle and shear stresses

The shaft rotates with 2456 rpm. The maximum performance is 103 kW whereas the average performance is 55 kW. The torsional angles, the shear stresses, and the safety factors were calculated for four different fibre layups which were chosen from Figure 12.

	torsional angle for normal load		torsional angle at peak load		calculated ultimate shear stress	safety factor for normal load	safety factor at maximum torsional moment	ultimate torsional moment (power)
	φ [rad]	φ [°]	φ [rad]	φ [°]	[N/mm^2]	—	—	[Nm]
H 40 A	0.2992	17	0.5592	32	417	9,8	5,2	2060
Thornel 75 S	0.2072	12	0.3872	22	218	5,1	2,7	1080
Thornel 75 S-E-Glas	0.2337	13	0.4367	25	194	4,6	2,4	960
Thornel 75 S-PRD	0.2300	13	0.4230	25	197	4,6	2,5	1000

Figure 13 Calculation of the shear stresses, results

Bending stresses

As the drive shaft is fixed on the tail by four bearings, it is forced to endure the deformation of the tail boom which causes a deflection of 1°20' in the normal bending case and of 2°20' at peak load. Figure 14 shows the distribution of the bending moments of the two regarded load cases.

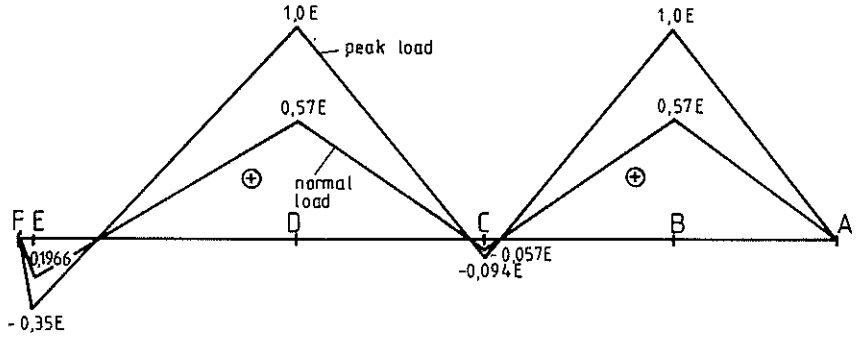

Figure 14 Plot of the bending moment of the drive shaft at different load cases as a function of the Young's modulus E (capital letters on bottom line indicate bearing positions)

It can be seen that both the moments and the bending stresses, resulting from them, increase if a fibre type with a higher Young's modulus is chosen.

The bending stresses as well as the shear stresses which are caused by the shear forces in the bearings and in the couplings are listed in Figure 15.

	Young's modulus 10^{-4} [N/mm²]	bending stress $\sigma_{N.L.}$ [N/mm²]	$\sigma_{P.L.}$ [N/mm²]	ultimate bending stress σ_{bu} [N/mm²]	safety factor N.L. [-]	P.L. [-]	maximum deflection f [mm]	maximum shear stress due to shear force $\tau_{N.L.}$ [N/mm²]	$\tau_{P.L.}$ [N/mm²]
M 40 A	6,16	14,1	24,8	387	27,5	15,6	106,1	0,63	1,13
Thornel 75 S	8,64	19,8	34,8	187	9,4	5,4	36,6	0,89	1,59
Thornel 75 S/E-Glas	8,63	19,8	34,8	194	9,8	5,6	37,9	0,89	1,59
Thornel 75 S/PRD	8,61	19,7	34,7	195	9,9	5,6	38,3	0,89	1,58

Figure 15 Calculated stresses due to bending

4.2 Coupling

Two different coupling types were analysed by means of the finite element programme NASTRAN:

a) filament wound coupling element with integrated flange

b) single disc coupling.

The structure was subdivided into quadrilateral shell elements (QUAD4 elements). Figure 16 shows a perspective view of the two analysed coupling types. For symmetric reasons, only one half of the couplings had to be idealized.

The same load cases as in the static tests of the couplings were regarded. As an example of the calculation, Figure 17 shows the deformation of the filament wound coupling element under bending moment. The load cases and a comparison between calculation and test results can be seen in chapter 9.

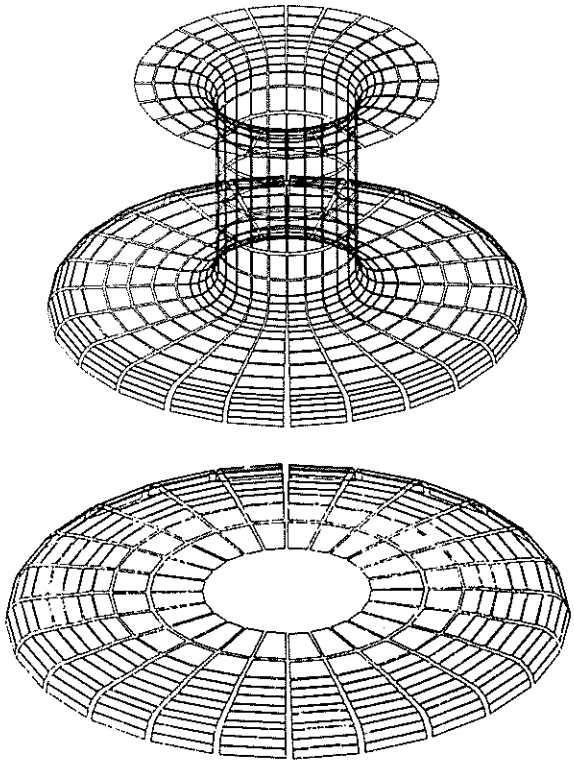

Figure 16 Idealization of two coupling types: above filament wound, below press-moulded (prepreg) coupling

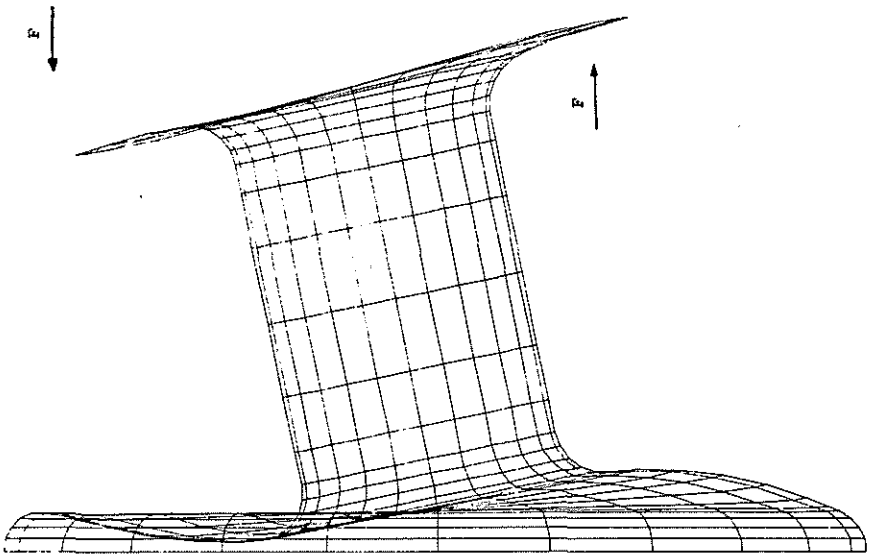

Figure 17 Bending of tht filament wound coupling element

5. Selection of the best solutions

In the chapters before the drive system has been regarded in a modular way. This was done because the best solution for the short drive shaft can differ from the best solution for the long drive shaft. This originates from the requirement for replacement of the bearings of the long drive shaft.

For the long and short shaft the design of the tube is the same. As can be seen from the results in chapter 4 concerning strength and stiffness and from the values given in Figure 8 the best solution for the tube is that one with the TORAY M 40-3000x40A fibre and 32 mm outer diameter. Not only natural frequency and stiffness but also the ultimate deflection is responsible for this selection. Under extreme flight conditions the long drive shaft makes deflections up to 89 mm. The tube out of TORAY M 40 fibre / epoxy is the only one that meets this requirement in addition to the other requirements. For the connection of the tube to the flange the bolted version 6 in Figure 4 has been selected for the long and the bonded version 1 for the short tube.

With reference to the couplings, the concepts 1, 5 and 6 in Figure 5 have been built and tested in order to judge the advantages and disadvantages of this three solutions in the field of manufacturing. Analytical results in chapter 4 showed that concept 1 is too stiff in tension and compression, whereas concept 5 and 6 are nearly equal from the analytical point of view. The main difference is in the manufacturing method. Concept 6 is produced by filament winding the part and curing it in a pressmould whereas concept 5 is produced out of prepreg sectors laid on a metal core and pressed in a die. This processes had influences on the test results. It has been shown that the reproducibility of the prepreg part was much better than of the filament wound part. Therefore, the concept 5 has been selected for further work.

The reasons led to three different test parts:

- short drive shaft with bolted flanges and a prepreg coupling at one end and a filament wound coupling at the other end - see Figure 18
- short drive shaft as described above but with an octagonal conical bonding between flanges and tube of the shaft - see Figure 19
- long drive shaft with bolted flanges and prepreg couplings at both ends. Areas for positioning the bearings on the CFC tube were doubled with GFC - see Figure 20

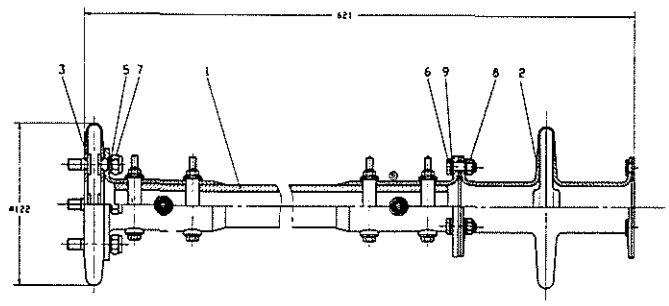

Figure 18 Test specimen 2, bolted version

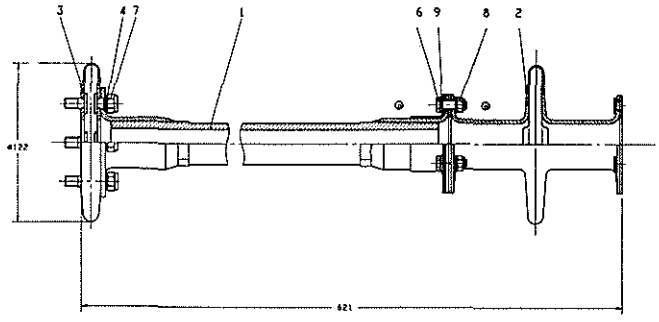

Figure 19 Test specimen 1, bonded version

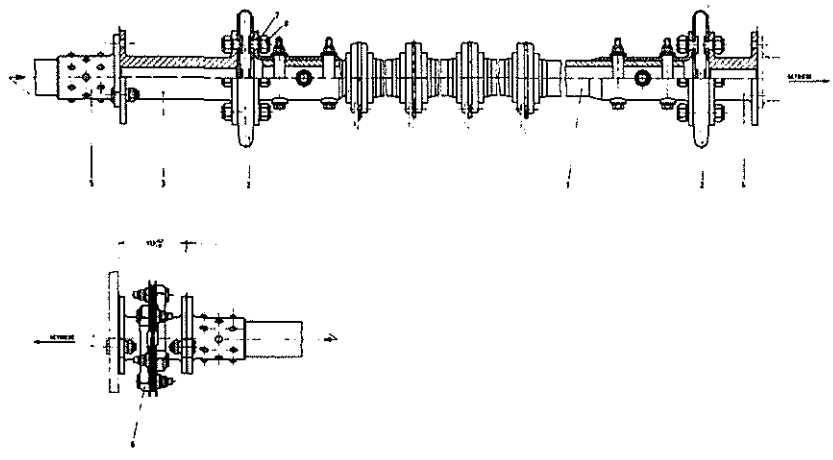

Figure 20 Long shaft, prototype test specimen

6. Design of the selected concept

6.1 Drive shaft

The CFC drive shafts are designed with TORAY M 40-3000x40A fibres bedded in CIBA CY209/HT972 epoxy resin with a fibre volume fraction of about 50%. The outer diameter is 32 mm and the wall thickness 5 mm. The laminate of the tube is composed of four layers in ±45° orientation with a thickness of 0.8 to 1.0 mm. The total thickness of torsional layers is 3.6 mm. Between these layers three unidirectional 0° bending layers with a total thickness of 1,4 mm are distributed. At each end of the CFC tubes the attachment zones for the flanges are seized by pressing the wet part before curing. For the octagonal 0.5° conical bonding zone the joining length is smaller than for the boltet version because it is determined by the necessary bonding area. CIBA AV138M/HV998 has been used as adhesive.

The precisely pressed area for the bolted version had an outer diameter of 32.0 mm (with a tolerance of -0.1 mm) over a length of about 80 mm. In this area six fitting holes of 10 mm diameter for the slotted spring type straight pins are located. For the long drive shaft at the positioning areas for the bearings a glass fibre fabric / epoxy composite acted as circumferential doubler. The same resin as for the CFC tube fabrication is used.

6.2 Load introductions to the flanges

The load introduction in the flanges from the shaft tubes are solved in two different ways:

- by shear strength of adhesive
- by bearing strength of bolted laminates.

The connections between couplings and flanges are realized only by bearing strength of the flange laminate. The detailed design can be seen in Figure 18 through 20. The laminate for this case consists of about 80% in ±45° orientation for the transfer of torsional loads and of additional 20% in 0°/90° orientation for improvement of bearing strength.

6.3 Coupling

The filament wound coupling (Figure 5, version 6) consists of E-glass-roving EC10-800-K43-CODE6913 and epoxy resin CIBA CY209/HT972 in fibre orientation ±45%. Going from the left to the right side of the coupling, the wall thickness varies from 2 mm in the flange side area to 3 mm in the tubular area of the flange side. From these 3 mm in the middle of the coupling the fibre orientation varies slightly to a sharper angle and with this the wall thickness reduces to 1 mm at the outer diameter and the middle of the coupling. In order to improve the bearing strength of the attachement areas to the flange a GFC doubler ring of 2 mm thickness with quasi-orthotropic fibre orientation is bonded on both ends of the coupling. The outer diameter of the coupling is 120 mm and the length is 134 mm. The part circle

diameter (PCD) of the attachment flanges is 60 mm with three fitting holes of 6 mm diameter.

The prepreg coupling is a hollow disc with variable wall thickness from inner to outer diameter. The wall thickness in the centre is 2 mm and in the area of the outer diameter 1 mm. The radial ring connecting the two walls of the disc has a curvature with 6 mm radius. At the PCD of each side of the coupling four titanium pins are incorporated in the composite in order to perform the connection to the drive shaft flange. The manufacturing and layup scheme of this GFC coupling are described in the next chapter.

The design of the tools for all these parts is not discussed in detail because of the limited space. It should only be mentioned that all tools are made of metal. The most interesting tool - for forming the interior shape of the prepreg coupling - is discussed in the following chapter.

7. Manufacturing of components

7.1 Drive shaft

Manufacturing method for the CFC drive shaft is a typical filament winding process. A precise cylindrical metal drum is fixed under tension load (especially for the long drive shaft) in the winding machine. For this special pretensioning devices have been designed to guarantee a minimum tension even under curing condition (120°C). After the bearing seats are turned to the exact diameter with a drill template holes for the flange connection are drilled.

7.2 Flanges

The flanges are built with structural prepreg containing E-glass fabric. The inner contour and exactness of the shape were the factors that mainly influenced metal tool design. This means that the inner surfaces have no mechanical treatment after curing. The flanges consist of different layers from which each is formed out of four sectors with a circular and rectangular part. On the layup a twopiece pressmould is positioned and pressed axially in a heated press. After the curing process the flanges are seized to length and the holes are drilled with drilling templates.

7.3 Coupling

In this chapter only the manufacturing of the prepreg version is discussed.

The material used for the composite part is the same as for the flanges. Titanium connection pins which are incorporated in the composite part have in their cylindrical part two straight areas in order to prevent turning of the pins during fastening of the coupling to the flange.

For the metal core on which the composite is laid, a material was necessary which can be removed from the part after curing without damaging it. A castable low melting metal alloy has been found for this purpose. At first, the machined titanium pins are fixed on each side of the mould shown in Figure 21. After this, the mould is closed and the casting of the metal starts. The casted core with fixed pins can be seen in Figure 21.

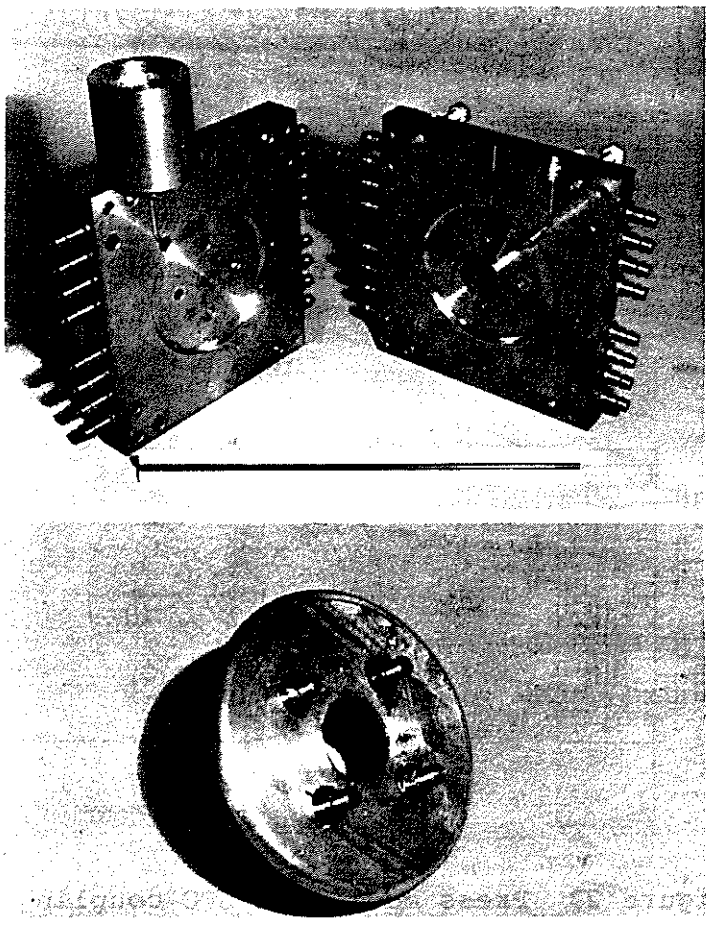

Figure 21 Mould and metal core with pins

This work is followed by applying a release agent on the surface of the core. Then, with the aid of punching tools and cutting templates single prepreg sheets for the coupling are prepared. They are positioned on the core according to the layup plan shown in Figure 22. The general method is close to that of flanges. After this layup two half metal rings are positioned on the outer diamter to form the exact radius of 6 mm. This configuration is then brought into the press mould (Figure 23). After curing at 100°C the GFC coupling with metal core is removed. Then the metal core is melted at a temperature of 130°C and the coupling is finished without any additional machining.

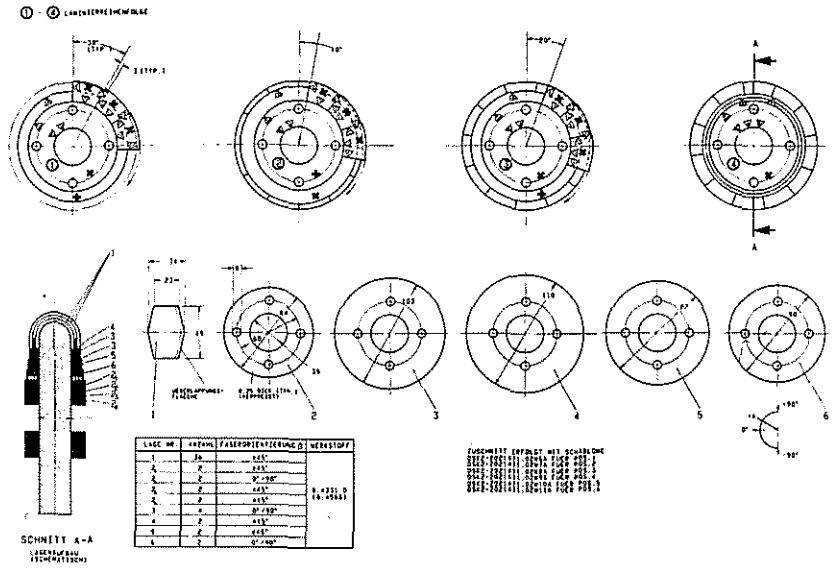

Figure 22 Layup plan for GFC coupling

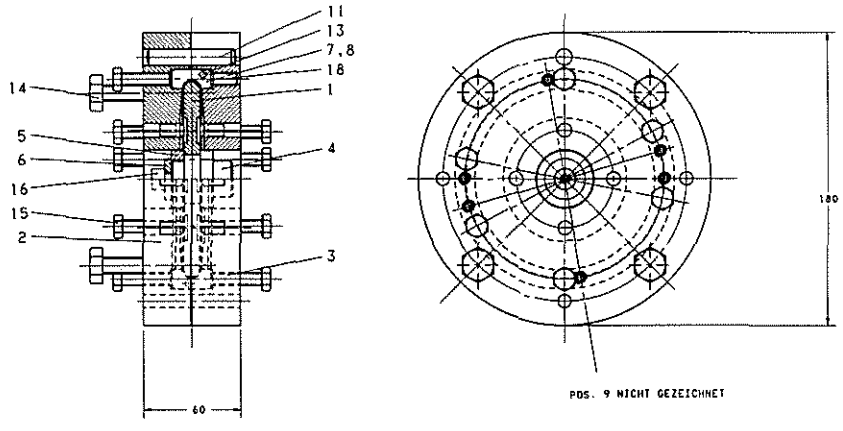

Figure 23 Press mould for GFC coupling

8. Testing

The tests can be divided in component tests and drive system tests. Component tests were performed statically. These tests concentrated on the coupling and the CFC tube. Stiffness tests for the coupling in bending, tension, compression, and torsion were done. The applied loads were in the range of the required loads - no ultimate tests were performed. These are foreseen after the dynamic tests in form of residual stiffness and strength tests. The obtained test results are compared with the analytical results in the following chapter.

Dynamic tests are performed on the short drive shaft specimen in form of start-stop-loads and additional permanent loads. Conditions under which the specimen were fixed in the test rig were

elongation per coupling + 1.3 mm

angle between each coupling and tube axis 1°.

Additionally, the following loads were applied in the 1st block:

A_1: start-stop-load:

1st step M_T = 160 ± 140 Nm, 20 cycles

2nd step M_T = 120 ± 110 Nm, 40 cycles

B_1: permanent load 2 hours at 2450 rev/min, M_T = 220 Nm

After the first block, which represents really acting loads was repeated 560 times (corresponding 1120 flight hours), the loads was increased in order to judge overload behaviour (e.g. M_T = 400 Nm).

No failure of shafts nor couplings was observed during these tests. The bolted flange, however, has to be redesigned, if higher loads come into account (increase wall thickness). Figure 24 shows the specimen in the test rig.

The long drive shaft with applied bearings and couplings was positioned in the test rig so, that each coupling had 1° deflection in axis, 1.3 mm tension and that one end of the shaft was fixed 50 mm above the other end (to simulate bending of the tail boom). Under this conditions a permanent torsional moment of 300 Nm at 2450 rev/min was applied for 500 hours.

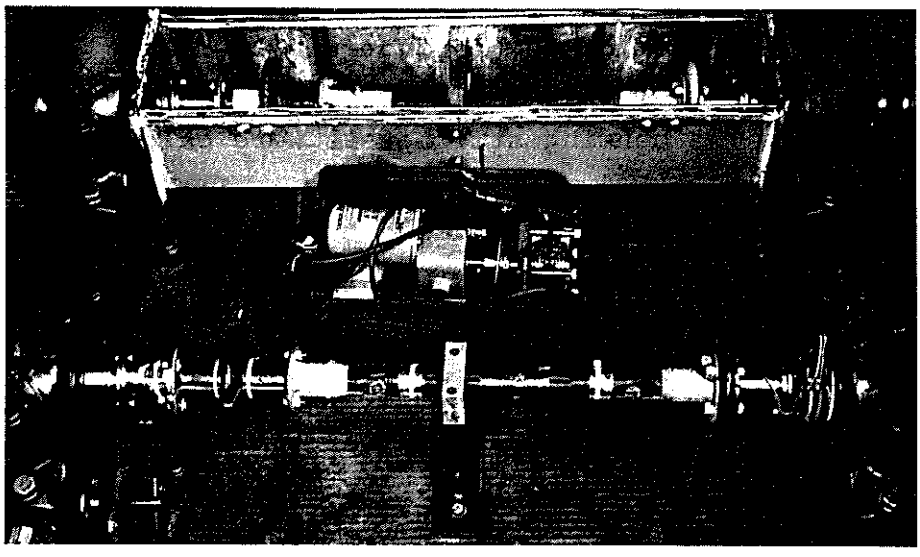

Figure 24 Short shafts in test rig

After this time the torsional moment was increased to 390 Nm for 240 hours. In Figure 25 the test rig with the specimen can be seen. Test results can be seen in the following chapter.

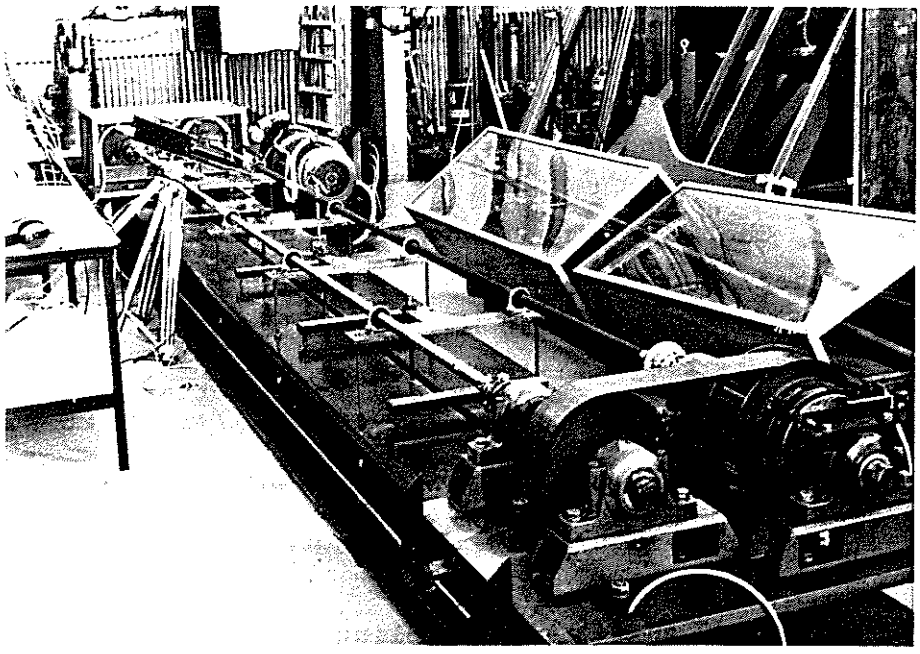

Figure 25 Long shaft in test rig

9. Comparison of analytical evaluation and test results

9.1 Static test results

Drive shaft

A shaft of about 300 mm length composed of the chosen M40A fibres and epoxy matrix was used for testing the drive shaft stiffness.

In order to determine the bending stiffness, the shaft was clamped at one side, and a force of 750 N was sequentially introduced at the free end in two radial directions (perpendicular to each other). The bending stiffnesses were calculated by means of the measured strains.

The torsional test was carried out with a torsional moment of 400 Nm.

Figure 26 shows the test results in comparison to calculated and required values.

	plant design	calculation	test
EI (bending) [Nm^2]	2460	2480	2480 1970
C_T (torsional springstiffness) [Nm/rad]	720	700	860

Figure 26
Stiffness of the drive shaft

It can be seen that the test results show a good correlation to the theoretical values.

Coupling

The stiffness tests of the composite couplings correspond with previously carried out tests of the production BO 105 metal version. The following loads were applied per coupling:

a) longitudinal elongation of ± 1.3 mm

b) angular deflection 1°

c) torsional moment of 390 Nm.

The couplings of type 1, 5 and 6 in Figure 5 were tested.

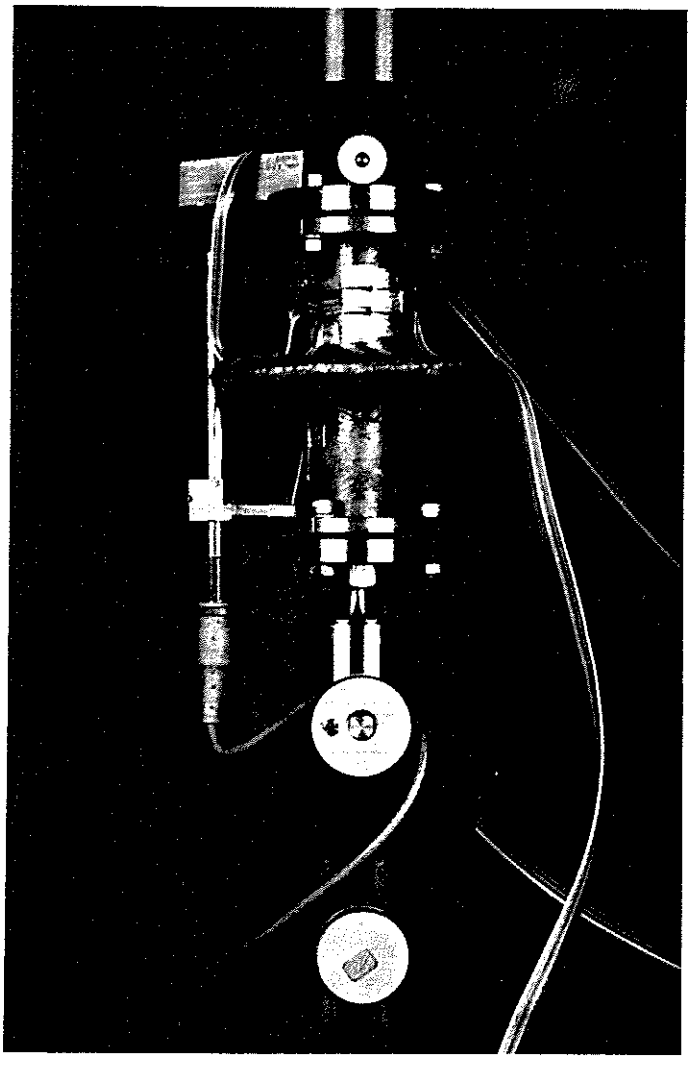

Figure 27 Filament wound coupling element, mounted for testing the longitudinal stiffness

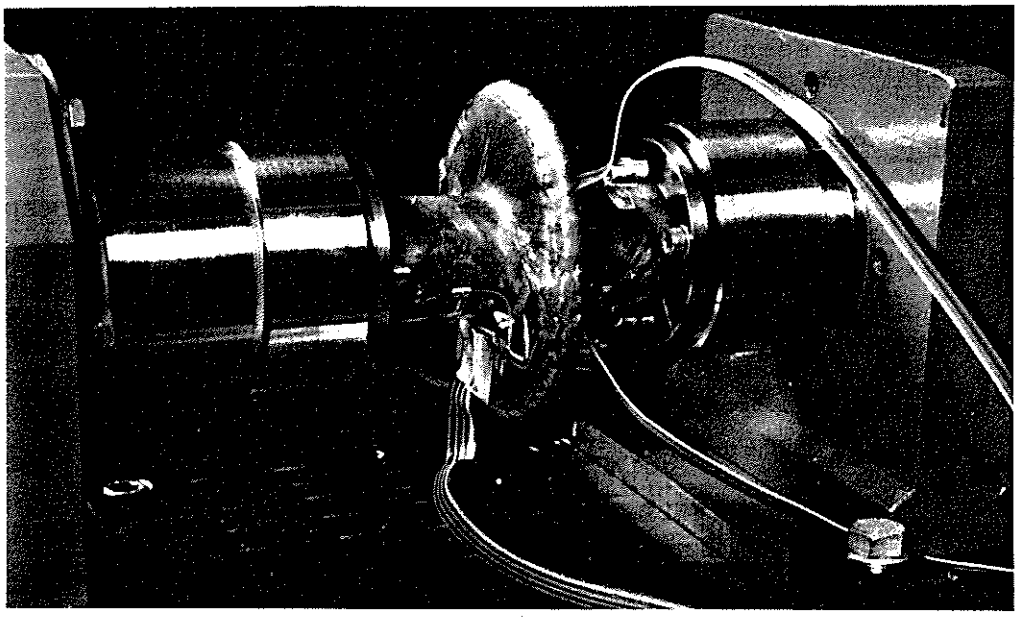

Figure 28 Filament wound coupling element, mounted for the torsion test; the right bearing is fixed, whereas the torsional moment is introduced at the loose left bearing

		spring stiffness in axial direction Nmm		bending stiffness $\cdot 10^3$ Nmm/rad	torsional stiffness $\cdot 10^6$ Nmm/rad
filament wound coupling with integrated flange	test	515		688	8,68
	calculation	300		500	7,66
prepreg laid coupling in two parts with integrated flanges	test	2200		not tested	not tested
single disc coupling*	test	324		499	35,6 79,0
	calculation	326		525	86,6
metal coupling with 10 lamellae	test	tension 22	pressure 461	118	14
metal coupling with 12 lamellae	test	43	540	198	16

Figure 29 Comparison of the test results and the calculation of the tested couplings

9.2 Dynamic test results

In order to prove the critical torsional and bending speeds for the manufactured prototype of the long TORAY HM fibre / epoxy

made tail rotor drive shaft, the equivalent dynamical systems shown in Figure 6 and 7 are used. The required stiffnesses of the CFC drive shaft have been determined experimentally. The results are for the torsional siffness 2559 Nm^2, for the bending stiffness 2405 Nm^2.

	I/kgm^2	$\omega/rad\ s^{-1}$	$k_T/Nm\ rad^{-1}$
tail rotor	0,94	232,5	-
tail rotor mast	-	232,5	20750
intermediate drive shaft (metal)	-	321	4900
long drive shaft (CFC)	-	256,8	640
front drive shaft (metal)	-	256,8	3660

Figure 30 Numerical values for the determination of the critical torsional speed

The BO 105 tail rotor driving system, modified by replacing the long steel shaft by the CFC shaft, yields a critical torsional speed ratio of 0.11 (over-critical operation). The lowest critical bending speed for the modified drive shaft is 1.65 referred to the operational speed (sub-critical operation). This evaluation is based on the numerical values summarized in Figures 30 and 31. In addition, the long CFC drive shaft has been operated up to the highest available speed on the tail rotor shaft test bench (about 130% of the rated speed). No resonance points were passed within the checked speed range.

	M/kg	M/kgm^{-1}	k/Nm^{-1}	$k_T/Nm\ rad^{-1}$	EI/Nm^2
front drive shaft (metal)	-	1,5	-	-	4390
long drive shaft (CFC)	-	0,6	-	-	2405
coupling (metal)	-	-	-	120	-
coupling (GFC)	0,3	-	-	470	-
supporting bearing	0,04	-	$3.1x10^6$	-	-

Figure 31 Numerical values for the determination of the critical bending speed

10. Economical aspects

The cost effectiveness of different versions is mainly influenced by the manufacturing costs of the parts, the number of single parts, and the mass of parts.

Therefore, after the manufacturing of the test parts, a certain basis was available for a cost comparison of the metal and the composite version. The production of parts for a number of 200 helicopters has been regarded. Obtained data for the costs of the metal version are set to 100%. The costs for composite parts are extrapolated from the costs of one part in prototype manufacturing. For the manufacturing of parts for 200 helicopters multiple tools are respected in the costs. The costs of the composite parts include 30% waist in prepreg within the material block. Results of this comparison are given in Figure 32. It can be seen that compared to the metal version a total cost reduction of 10% for the composite parts can be expected.

Basis: Parts for 200 helicopters						
Component	Total costs [%]		Material costs [%]		Manufacuring costs [%]	
	Metal	Composite	Metal	Composite	Metal	Composite
1 drive shaft incl. 2 flanges without bearings	46	69,3	33,8	29,9	12,2	39,4
2 couplings	52,2	20,3	30,0	8,0	22,2	12,3
assembly	1,8	0,4	0,5	0,4	1,3	--
Σ	100,0	90,0	64,3	38,3	35,7	51,7

Figure 32 Cost comparison of metal and composite version

As the next important points the mass of parts and the number of parts were investigated. Figure 33 illustrates these data for the metal and the composite version of long and short tail rotor drive shaft. It is shown that for the long drive shaft a mass reduction of about 4 kg and an additional reduction in the number of parts of 26 is possible. The short drive shaft shows a mass reduction of about 1 kg and a reduction in the number or parts of 64. The great amount at the reduction in the number of parts for the short drive shaft arises from the fact that on this shaft two couplings are attached.

Part	Mass [g]			Number of parts		
	Metal	Composite	Mass reduction	Metal	Composite	Parts reduction
Long tail rotor drive shaft (l=3940) with a coupling on one side and a flange on the other and additional 4 bearings	7780	3730	4050	80	54	26
Long tail rotor drive shaft (l=3940) with a coupling on one side and a flange on the other without bearings	6980	2930	4050	72	46	26
Short tail rotor drive shaft (l=731) with a coupling on each end of the rod	1930	860	1070	101	37	64

Figure 33 Tail rotor drive system: mass and number of parts comparison of metal version versus composite version

Figure 34 shows drastically that the reduction in the number of parts in the coupling is responsible for the high efficiency of the short composite drive shaft.

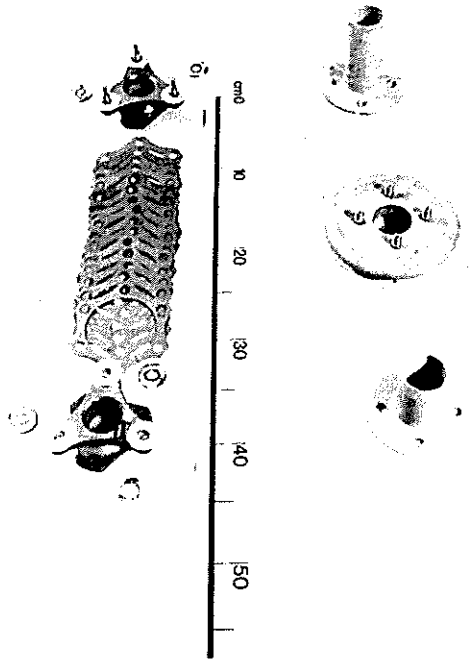

Figure 34 Comparison of the number of parts for composite and metal coupling

11. Next programme steps

In addition to the dynamic tests the residual stiffness and strength of the couplings and tubes which passed the tests are intended to be checked.

After this, dynamic tests with a greater number of components must be performed in order to substantiate the basis for flight tests over a longer period.

12. Conclusions

The obtained test results for the designed bolted and bonded versions of the CFC-tubular drive shafts with GFC couplings are very encouraging. Although the GFC flange for the bolted version has to be redesigned it could be shown that this is a good solution for the long drive shaft. The bonded solutions for the short drive shaft passed all tests without any failure during about 1200 simulated flight hours. During this time no GFC coupling nor CFC shaft failed. The elastic behaviour of the GFC coupling could be improved compared to the metal version: higher torsional and lower compression stiffness. The bending and tension stiffness, however, are higher than the ones of the metal version, which is a slight disadvantage.

Discussing the test results in terms of flight hours, it can be stated that the results according to permanent loads correspond to 1200 flight hours. The start-stop-loads that have been successfully passed represent 2400 flight hours.

Regarding the economical aspect of the composite version, it has been shown that a manufacturing cost reduction of 10%, a mass reduction of 4 kg for the long shaft and 1 kg for the short shaft and a reduction in the number of parts is possible.